3.3. Texture formation

The orientation of the 2212 grains was random in the initial stage, but only grains oriented parallel to the substrate could grow to a size exceeding the film thickness, because either the substrate or the film surface (surface-tension) acted as growth barriers. Some of the initially misoriented grains were turned into a parallel position during growing, while others remained misoriented forming obstacles for the superconducting current flow. Some grains, which were oriented almost perpendicular to the substrate, grew inside the silver substrate.

The reason for the highly aligned microstructure in Bi-2212 thick films can, therefore, be found in the extreme two-dimensional growth of the Bi-2212 grains in combination with the limited thickness of these samples. This alliance forces the grains to grow with their c-axis perpendicular to the substrate.

4. Acknowledgments

The authors gratefully acknowledge the financial support of the Schweizer Nationalfonds (NFP 30).

5. References

[1] B. Heeb et al., *J. Mater Res.*, **7** (11) 2948 (1992).
[2] J. Kase et al., *IEEE Trans. Mag.*, **27** 1254 (1991).
[3] Th. Lang et al., *Proc. for the 4th World Conf. on Supercond.*, Orlando FL, USA, June 27-July 1, (1994), in press.
[4] D. Buhl et al., *Proc. for the 4th World Conf. on Supercond.*, Orlando FL, USA, June 27-July 1, (1994), in press.
[5] R.D. Ray II, *Physica C*, **175** 255 (1991).
[6] R. Müller et al., *Physica C*, **243** 103 (1995).
[7] J. Shimoyama et al., *Adv. in Superconductivity V*, Eds. Y. Bando and H. Yamauchi, Springer Verlag Tokyo, 697 (1993).

Inst. Phys. Conf. Ser. No 148
Paper presented at Applied Superconductivity, Edinburgh, 3–6 July 1995

Texturing of (2223) superconducting Bi-Pb-Sr-Ca-Cu-O ceramics by different processes using hot pressing and melting in a magnetic field

J.G. Noudem[1], J. Beille[2], D. Bourgault[1], E. Beaugnon[1], R. Tournier[1], D. Chateigner[3], P. Germi[3], M. Pernet[3].

(1) EPM-MATFORMAG, (2) Laboratoire Louis Néel, (3) Laboratoire de Cristallographie, C.N.R.S., B.P. 166, 38042 Grenoble, cedex 9, France;

Abstract : We compare several ways of texturation of superconducting (2223) Bi-Pb-Sr-Ca-Cu-O, namely hot pressing (HP), magnetic melt texturation (MMT) and an original method combining the two processes (MMHPT). Different degrees of texturation are compared from scanning electron microscopy observations and X-Ray diffraction spectra including pole figures, as well as physical characterizations based on electrical transport measurements. We analyze the relative effects of several parameters of the process : temperature, stress and magnetic field.

1. Introduction

Bi-Pb-Sr-Ca-Cu-O ceramics are interesting in view of their high critical temperature and the platelet shape of their constituting grains, which makes them easy to orientate. Their weak point is their sensitivity to magnetic field, due to a weak intrinsic pinning of the vortices in the (a,b) planes in line with their 2 D character, and to the importance of parasitic phases, especially for the (2223) phase. For industrial applications, it is important to process ceramics with oriented grains, in order to insure a better connexion between them, and to improve the intergranular medium.

In previous works [1,2], we have applied several ways of texturation of superconducting (2223) Bi-Pb-Sr-Ca-Cu-O ceramics : hot pressing (HP), magnetic melt texturation (MMT) and an original method combining the two last processes (MMHPT). In this paper, we compare the superconducting characteristics of the samples processed in the different techniques and discuss the effects of the various parameters : temperature, magnetic field, pressure.

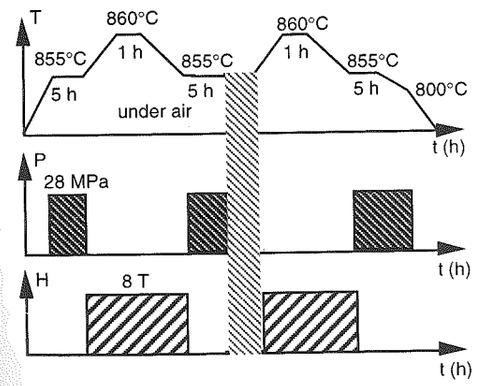

Figure. 1. Cycles of temperature, pressure and magnetic field.

2. The different processes of texturing the (2223) Bi-Pb-Sr-Ca-Cu-O ceramics

We used magnetic susceptibility measurements at high temperature to determine the begining and the end of melting [2].

A high pressure of 28 MPa is applied for 5 hours at a maximum temperature of 855°C, just above a magnetic susceptibility minimum ascribed to the beginning of melting. In the magnetic melt texturation, a magnetic field of 8 tesla is applied from the beginning until the end

of the processing. A maximum temperature of 860°C is established for 1 hour and then slowly decreased down to 700°C at a cooling rate of 1°C/hour. The parameters of the hot pressing technique have been previously optimized [1]. In our original (MMHPT) process, a pressure of of 28 MPa is applied for 5 hours while the temperature is kept constant at 855°C.

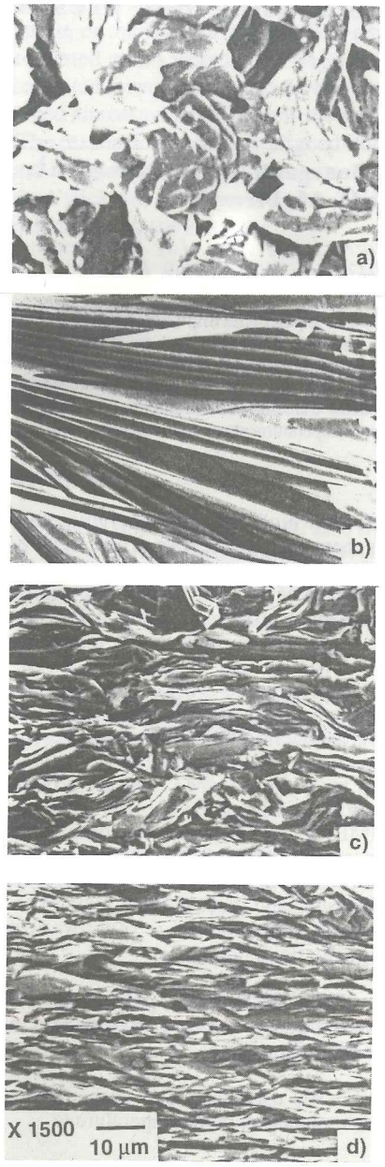

Figure. 2. SEM micrograph pictures of a face broken parallely to the applied stress and magnetic field direction for the different texturing processes.

Pressure is then released, the magnetic field is turned on and the temperature is increased up to 860°C, maintained 1 hour and then decreased at 1°C/hour down to 855°C where the magnetic field is turned off and pressure reapplied for 5 hours. The proposed cycle thus includes an initial hot pressing step, followed by melting step under magnetic field, and ending with a hot pressing step. The three cycles of temperature, pressure and magnetic field of this process may be repeated several times, as illustrated in Figure. 1,which should increase the performances of the sample.

3. Physical characterizations

3.1. Scanning electron microscopy (SEM):

SEM pictures of faces broken parallely to the axis of the texturing parameter (Figure. 2) cleary show different effects induced by these processes : a) classical sintering, b) magnetic melt texturation, c) hot pressing, d) hot pressing combined with magnetic melt texturation.
Figure 2a shows no preferential orientation of the constituting platelets ≈ 20 µm in size, whereas figure 2b indicates a preferential orientation of the platelets perpendicularly to the magnetic texturing field with i) a larger size of the platelets (> 50 µm), ii) a sizeable dispersion in the c axis directions, iii) quite large voids between grains. Figure 2c shows a higher density, but the platelets have a wavy shape and a reduced size probably due to mechanical defects: Figure 2d shows there is a good alignement of the platelets which appear very well compacted, their wavy aspect being largely reduced.
From these observations, we conclude that melting in a magnetic field is favorable to the growth of large, oriented cristallites, but with loose connections and voids in between. We suggest that the first hot pressing step of our MMHPT process prealigns the platelets, magnetic field favors the growth of orientated grains. Finally, while the stay in the liquid state in a the consecutive second hot pressing step confers a high density to the material.

3.2. Pole figures

Since classical Θ-2Θ X ray partterns revealed intense 00l reflections for a MMHPT Bi-2223 surface perpendicular to the applied magnetic field and uniaxial stress, we operated pole figure measurements on this type material. We used the Schulz reflection geometry [3] with monochromatic Cu(Kα) radiation.
The pole figures were corrected for background and defocusing [4] and then normalized [5] in order to calculate the distribution density of the crystallites. This value is normalized to 1 m.r.d. (multiple of random distribution) for a perfectly untextured sample. In the following χ is the tilt angle of the Schulz geometry.
According to our elaboration process, we do not expect any in-plane orientation. We first verified this fact on the {115} pole figures (not shown here) which present a ring of strong intensities centered on χ = 60°, the theoretical value of a single Bi-2223 crystal.
Figure. 3 is the {00$\underline{14}$} pole figure of the sample parially melted at 860°C which exhibits the strongest critical current density of Jc = 3800A/cm^2 obtained. This figure shows that {00l} normals are not dispersed by more than 25° from the fiber axis (magnetic field and uniaxial stress direction), taking reference at 15 % of the maximal intensity on the figure. The maximal density for this reflection is 4.5 to 5 m.r.d. No variation of the texture degree has been observed between the core of this sample and the interface with the rod. We also observe on this figure a ring beginning at χ = 65° which has not been measured further than χ = 72°. This ring corresponds to the {020}/{200} contribution located at a sufficiently proach Θ value, observable by defocusing at the Θ_{0014} position. Taking into account misalignments occuring from the positionning of the sample on the goniometer and from the magnetic field and uniaxial stress sample axis positionning, this {020}/{200} contribution proves the a and b random orientation around c axis.
We analyzed the {00$\underline{14}$} pole figure of the sample partially melted at 865°C on which we measured Jc = 2000 A/cm^2. This pole figure indicates a dispersion of the {00l} plane normals up to 30°, with the same reference as above and consequently the orientation density is lowered to 3.5-4 m.r.d. at the maximum. This texture loss compared to with the previous sample, and the presence of parasitic phases both contribute to decrease the Jc.

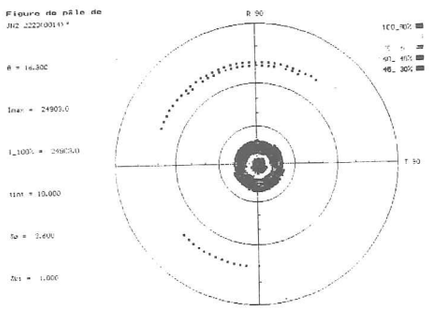

Figure. 3. {0014} X-ray pole figure of the sample partially melted at 860°C.

3.3. Electrical transport measurements

These sample processes can be classified based on increasing transport critical current densities Jc (77 K, 0 T) as : a) classical sintering (Jc ≈ 800 A/cm^2), b) MMT-process (1500 A/cm^2), c) HP-process (Jc ≈ 2500 A/cm^2) and d) MMHPT-process (3800 A/cm^2)

The effect of the magnetic field applied during the process is highlighted by considering samples prepared by MMHPT without magnetic field, but with the melting step at 860 °C, which gives a Jc of only 2500 A/cm^2.

Figure. 4a shows an increase of critical current density Jc versus critical temperature Tc for samples elaborated according to the MMHPT process at various partial melting temperatures as usually observed.

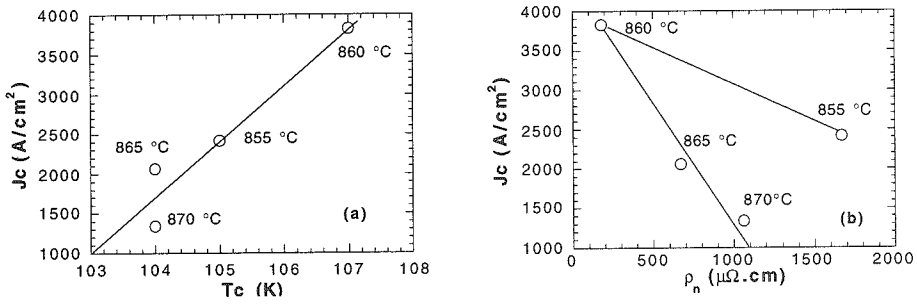

Figure. 4. Plots of Jc a) versus Tc b) versus ρ_n.

In Figure. 4b the critical current density Jc of the same samples is plotted versus the normal state resistivity ρ_n, and shows two different regimes. For partial melting temperatures higher than 860 °C, a decrease in Jc correlates with and increase in ρ_n, attributed to a larger proportion of parasitic phases. Below 860 °C, a decrease in the temperature of the melting dwell correlates with a decrease in Jc and with an increase in ρ_n . In that case, the proportion of the liquid phase is too small to allow rotation and growth of the platelets as well as their densification. Nevertheless, ρ_n increases due to a lowering of the temperature of the upper dwell, which little affects the Jc. The defects induced by hot pressing alone may act as pinning centers for the vortices. Consequently, it is better to be a little below the optimum partial melting temperature than above.

4. Conclusion

The process of partial melting in a magnetic field combined with hot pressing (MMHPT) allows to produce very dense ceramics of Bi-Pb-Sr-Ca-Cu-O with a better degree of texture than those obtained by hot pressing or melting in magnetic field. However, the temperature window for melting under field is very narrow and has to be carefully controlled. If this temperature is too low, there is no extra effect compared to hot pressing only, if it is too high, melting induces parasitic phases which strongly depress the superconducting performances. Once the difficulty of temperature control is mastered, the process is interesting for the production of large samples with critical current densities above 3800 A/cm^2.

Acknowledgments

J.G.N acknowledges his followship from ADEME and Alcatel Alsthom. M. Bonvalot is warmly thanked for useful discussions and very careful reading of the manuscript. We are grateful to P. Amiot for her help in carrying out the SEM studies.

references

[1] J.G. Noudem, J. Beille, D. Bourgault, A. Sulpice and R. Tournier : Physica C. **230** (1994) 42.
[2] J.G. Noudem, J. Beille, D. Bourgault, E. Beaugnon, A. Sulpice, R. Tournier, D. Chateigner, P. Germi and M. Pernet : to appear to Supercond. Sci. Technol. **8** (1995) 558..
[3] L.G. Schulz : J. Appl. Phys. **20** (1949) 1030.
[4] J.C. couterne and G. Cizeron : J. Appl. Cryst. **4** (1971) 461.
[5] J.R. Holland : Adv. X-Ray anal. **7** (1964) 86.